



## Performance estimation and optimization of an adiabatic H<sub>2</sub>O-LiBr absorption system using artificial neural networks

## Estimación de desempeño y optimización de un sistema de absorción adiabático H<sub>2</sub>O-LiBr usando redes neuronales artificiales

Gutiérrez-Urueta Gedy Luz

Universidad Autónoma de San Luis Potosí  
Facultad de Ingeniería, San Luis Potosí, México  
E-mail: [gedy.gutierrez@uaslp.mx](mailto:gedy.gutierrez@uaslp.mx)  
<https://orcid.org/0000-0002-4314-8254>

Colorado Darío

Universidad Veracruzana  
Centro de Investigación en Recursos Energéticos y Sustentables  
E-mail: [dcolorado@uv.mx](mailto:dcolorado@uv.mx)  
<https://orcid.org/0000-0003-4157-1005>

Hernández José Alfredo

Universidad Autónoma del Estado de Morelos  
Centro de Investigación en Ingeniería y Ciencias Aplicadas (CIICAp), Cuernavaca  
E-mail: [alfredo@uaem.mx](mailto:alfredo@uaem.mx)  
<http://orcid.org/0000-0002-2107-3044>

Rodríguez-Aumente Pedro

Universidad Carlos III de Madrid (UC3M)  
Departamento de Ingeniería Térmica y de Fluidos. Leganés, Madrid  
E-mail: [aument@ing.uc3m.es](mailto:aument@ing.uc3m.es)  
<https://orcid.org/0000-0002-6966-1451>

Rivera Wilfrido

Universidad Nacional Autónoma de México  
Instituto de Energías Renovables, Morelos  
E-mail: [wrgf@ier.unam.mx](mailto:wrgf@ier.unam.mx)  
<https://orcid.org/0000-0002-9845-5542>

### Abstract

The search for alternatives to curb climate change and its devastating consequences for today's society, leads to research environmentally friendly climate systems. To optimize or control them, artificial neural networks (ANN) is considered an effective option. Adiabatic absorption is based on separate design for heat and mass transfer process in order to reduce the size of equipment. This study deals with the application of ANN on the experimental results of a single effect water-lithium bromide adiabatic absorption facility and its optimization using an inverse ANN. Transient and steady state data were used to obtain three empirical models. The models developed correspond to the coefficient of performance (COP), cooling power and generation power of the facility. Steady state statistics consists of 219 experimental points obtained at different operating conditions. These data were used to train and test the steady state and transient ANN models. For transient statistics, 1445 values were considered for a period. In the validation data set, the results showed that simulations and the experimental data were in good agreement with an  $R > 0.98$  for both steady state and transient models. A model for COP, based on the principle of accessibility of data, was developed including temperatures for the external fluid circuits with good results. The inverse neural model applied to transient data demonstrated satisfactory results as well, making possible the optimization of the facility. These results illustrate the adequacy in using an ANN with transient data in absorption systems, making it especially attractive for solar cooling applications.

**Keywords:** Adiabatic absorption, water-lithium bromide, absorption systems, artificial neural network, performance estimation, optimization.

### Resumen

La búsqueda de alternativas para frenar el cambio climático y sus consecuencias devastadoras para la sociedad actual, conduce a la investigación de sistemas climáticos respetuosos con el medio ambiente. Para optimizarlos o controlarlos, las redes neuronales artificiales (ANN) se consideran una opción efectiva. La absorción adiabática se basa en un diseño separado para el proceso de transferencia de calor y masa con el fin de reducir el tamaño del equipo. Este estudio trata la aplicación de redes neuronales artificiales (RNA) sobre los resultados experimentales de un sistema de absorción simple efecto agua-LiBr y su optimización utilizando una red neuronal inversa. Se usaron datos tanto en estado transitorio como estacionario para obtener tres modelos empíricos. Los modelos desarrollados corresponden al coeficiente de rendimiento (COP en inglés), potencia de refrigeración y de generación de la instalación. Las estadísticas de estado estable consisten en 219 puntos experimentales obtenidos en diferentes condiciones de operación. Estos datos se utilizaron para entrenar y probar los modelos de estado estacionario y transitorios de ANN. Para las estadísticas transitorias, se consideraron 1445 valores para un período. En el conjunto de datos de validación, los resultados mostraron que las simulaciones y datos experimentales se ajustan con un  $R > 0.98$  para ambos modelos, transitorio y estable. Se obtuvo un modelo para el COP, con base en la accesibilidad de los datos, incluyendo temperaturas de los circuitos de fluido externos con buenos resultados. El modelo de red neuronal inversa aplicado a los datos transitorios demostró resultados satisfactorios, haciendo posible la optimización de la instalación. Estos resultados ilustran la idoneidad del uso de una RNA con datos transitorios en sistemas de absorción, lo que es especialmente atractivo para aplicaciones de refrigeración solar.

**Descriptores:** Absorción adiabática, agua-Bromuro de litio, sistemas de absorción, redes neuronales artificiales, estimación de desempeño, optimización.

## INTRODUCTION

The use of absorption systems represents an option for the substitution of organic refrigerants with natural substances and a reduction in electricity consumption. This fact, as well as the possibility of using solar energy as the input power, has led to an increased interest in the introduction of absorption systems in air conditioning and refrigeration applications.

The improvement of heat and mass transfer processes is a key factor in the reduction of the exchange area and size of the absorber that in turn, allows for the reduction of weight, volume and cost of the absorption equipment. The basis for the development of adiabatic absorption runs along the same line: if the concentrated solution is sub-cooled, i.e. its temperature is reduced below the equilibrium temperature at the current concentration, and then distributed on the refrigerant vapour into an adiabatic chamber, the refrigerant vapour is then absorbed by the solution. Once the absorption process begins, the solution is diluted and its temperature increased because of the transformation of vapour into liquid. The processes of heat and mass transfer are then separated into two different pieces of equipment. The process of cooling the solution is moved out of the absorber into small dimension heat exchangers thus reducing the heat transfer area. When this absorption method is used, part of the solution that leaves the absorber has to be sub-cooled and re-circulated to the absorber, with the purpose of reaching the final concentration required for the diluted solution. The other part is then pumped to the generator to be concentrated again.

In general, a separate design of sub-cooler and absorber allows for a better optimization of each component, helping to improve the overall efficiency. This is why adiabatic absorption is being researched as one method for improving absorption processes by separating and individually optimizing absorption and heat rejection and is also the base for the development of the equipment here presented.

One field of interest in absorption systems is the prediction and control of their performance. This is done through the development of models or calculation methods that analyze the performance of an absorption cycle (Hellmann *et al.*, 1998; Joudi and Lafta, 2001; Florides *et al.*, 2003). In this sense, artificial neural networks (ANN) are a very attractive application due to increasing interest in their use in load forecasting, refrigeration, and modeling of heat pump systems (Arcaklioglu, 2004; Mohanraj *et al.*, 2009; Hosoz and Ertunc, 2006; Laidi and Hanin, 2013). State of the art studies, both theo-

retical and experimental concerning the use of ANN were well resumed by Mohanraj *et al.* (2012). It is particularly interesting if applied to absorption cycles, given the fact that performance parameters are affected by a number of variables, like temperatures and flow rates, varying simultaneously during the operation.

For the particular case of absorption system modelling using ANN, some works can be summarized: various papers have been devoted to the modelling of the thermodynamic properties of the most commonly used fluids in absorption systems (Sözen *et al.*, 2004b; Şencan, 2007; Şencan *et al.*, 2006; Şencan and Kalogirou, 2005; Sözen and Akçayol, 2004a; Sözen *et al.*, 2003). They also show results regarding the system performance using the ANN results. The modelling of a steam fired double effect absorption chiller in a cooling process, used in the pharmaceutical industry, is presented by Manohar *et al.* (2006). This study also uses an ANN based on external cooling and chilled water temperatures, with good predicting results. Chow *et al.* (2002) combine a neural network and genetic algorithms for the controlled optimization of a direct-fired absorption system. The system-based controlled approach optimizes the use of fuel and electricity for the economical operation of a commercial absorption unit, concluding that considerable savings can be achieved. Yung (2007) reported the optimal chiller sequencing in a semiconductor industry by applying ANN to the power consumption data. The results showed that the electricity consumption could be reduced varying the chillers start-up sequencing. More recent papers include: the work performed by Rosiek and Batlles (2010) on the use of ANN to model a solar-assisted air-conditioning system. This system is based on a commercial single-effect LiBr-H<sub>2</sub>O absorption chiller fed by water coming from solar collectors. Using real data, they obtained a model to predict the efficiency of both chiller and the global system, giving a list of key variables. Labus *et al.* (2010) compared different methods for modeling the performance of a small capacity absorption chiller, concluding that an ANN was slightly better than other models analyzed. Hernández *et al.* (2012) used an inverse ANN in order to estimate the performance of a solar intermittent refrigeration system for ice production under different experimental conditions, showing optimization in performance and a sensitivity analysis. Labus *et al.* (2012) proposed a controlled strategy for a commercial absorption cooling system by taking the temperature and flow rates of external circuits. They used an inverse ANN in order to achieve the desired controlled strategy with good results. Hernández (2009a) developed a estimation for predicting operating conditions of variables,

depending on a desired response variable based on a neural network inverse. The mathematical development describes the use of Nelder-Mead-Simplex method to solve the formulation and obtain the optimum operating conditions on heat and mass transfer during foodstuffs drying. Álvarez *et al.* (2016) developed an ANN for the modelling of the performance of a horizontal falling film absorber with aqueous (lithium, potassium, sodium) nitrate solution. The authors reported that the ANN model was an effective tool for predicting the efficiency parameters of the absorber. Kumar *et al.* (2016) reported the use of ANN integrated with genetic algorithm to predict the performance of direct expansion solar assisted heat pump. The results showed that the use of ANN integrated with GA gives better optimized values compared to the value obtained from ANN. Afram *et al.* (2017) carried out a comprehensive review of the ANN based model predictive control for systems design. Tugcu and Arslan (2017) developed a model to optimize an absorption refrigeration system using  $\text{NH}_3\text{-H}_2\text{O}$  driven with geothermal energy. The optimum designs were determined using the obtained weights and biases of the best ANN topology, yielding a coefficient of performance and exergy efficiency of 0.57 and 0.62, respectively.

The use of inverse ANN has been successfully applied to predict the optimal operation conditions for a single-stage heat transformer (Colorado *et al.*, 2011), the optimum coefficient of performance of a heat trans-

former (Morales *et al.*, 2015) and polygeneration systems (Hernández *et al.*, 2013) among others.

From the above summary, it can be concluded that the application of inverse ANN on an adiabatic absorption system under transient conditions, using original experimental data, has not yet been explored. The transient model focuses on the importance of accounting for the time-varying operation conditions. This study presents the prediction of the performance variables of a particular test facility, based on the concept of adiabatic absorption and its optimization using an inverse ANN. The experimental data available was used to create a model with predicting purposes. Three ANN models for the prediction of evaporator and generator powers, as well as *COP* were developed, all with good accuracy and short computation time.

## DEVELOPMENT

### SYSTEM DESCRIPTION

Figure 1 shows a diagram of the single effect absorption test equipment. It consists of four loops: the hot loop, the solution loop, the cold loop, and the chilled water loop. Main components include: two evaporators, absorber, generator, condenser, sub-cooler and solution heat exchanger. The last four components are plate heat exchangers while the evaporators are fan-coiled tubes and the absorber is an adiabatic chamber. A computeri-

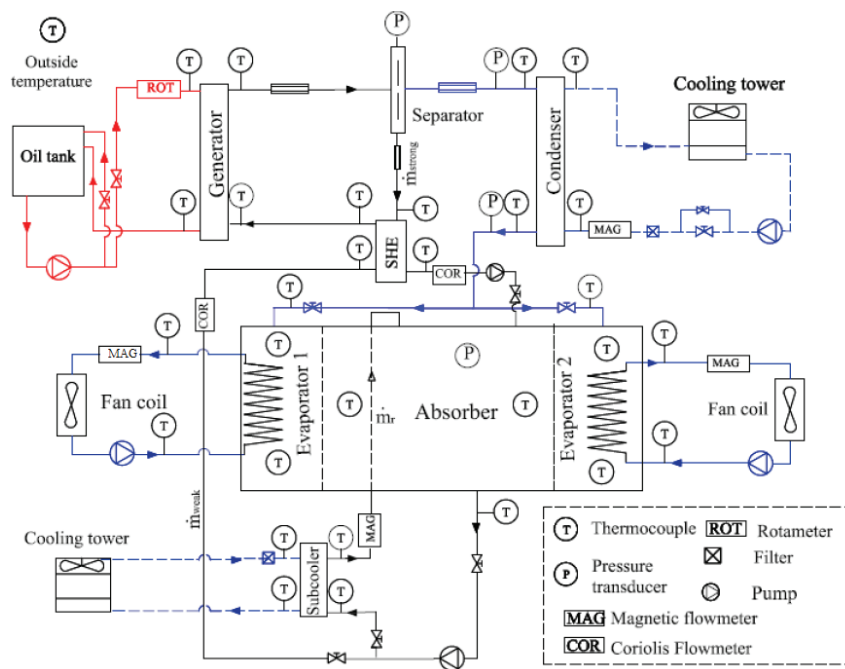


Figure 1. Flow diagram of the test facility

zed data acquisition system is used to register the measured data.

Aqueous LiBr solution inside the absorption chamber flows into two separate streams: a strong solution (solution poor in water or concentrated solution) coming from the generator, and a re-circulated solution. The strong solution is separated from the water vapor, which goes to the condenser, and directed to the absorber. A re-circulated solution is extracted from the bottom of the absorption chamber and pumped into the sub-cooler, where most of the absorption heat is rejected and then the sub-cooled solution is returned to the absorber. Two fan coils receive the external fluid circulating through each evaporator. The objective of placing two evaporators is to have a larger heat exchange area available and to guarantee the symmetry in the supply of vapor to the absorption vessel. Distribution problems in the refrigerant flow were detected; which will be discussed in following sections.

The experimental setup configuration and the experimental uncertainty analysis were described in detail in other publications (Gutiérrez *et al.*, 2006; Gutiérrez *et al.*, 2011). Figure 2 illustrates the experimental test facility.

#### EXPERIMENTAL TEST RUN

The data acquisition system is composed of two data-loggers, manufactured by Yokogawa, with 50 input ports available altogether, and a 24 V power supply. The oil flowmeter and the pressure transducers use the power supply to output an electric current of 4 to 20 mA. The input ports were read in intervals of 0.5 seconds.

The experimental procedure consists of periods of start-up, normal operation, and shut down of the machine. Start-up begins with the heating of the thermal oil from ambient temperature to the temperature set point  $t_{set}$  while the oil is pumped to the generator. The solution pump is switched on and the weak solution flow rate  $\dot{m}_{weak}$  to the generator is fixed at the desired value changing the frequency of the pump and adjusting the valves. The re-circulated solution flow rate  $\dot{m}_r$  varies according to the aperture of the valves and the driving frequency of the pump engine. Cooling tower flows are also switched on at this moment. Table 1 shows the operating ranges of the controlled parameters and of the variables considered in the study.

Figure 3 indicates the time period until stability is achieved (time elapsed until equilibrium). Some variables are plotted against time in order to show their evolution during a typical experiment. These variables are: inlet oil temperature,  $T_{oil,i}(t_{set})$ , outlet solution temperature at generator,  $T_{G,o}$ , outlet chilled water temperatures

at evaporators 1 and 2,  $T_{chw1,o}$  and  $T_{chw2,o}$ , mass flow rates and salt concentration of weak and strong solutions  $\dot{m}_{weak}$ ,  $\dot{m}_{strong}$ ,  $X_{weak}$  and  $X_{strong}$ . The fluids in the machine are initially at ambient temperature. The start up of the machine is represented by an increasing tendency of the variables, until the set value of generation temperature (in red,  $T_{oil,i}$ ) is reached. Then, indicated with a circle, the stability is reached.

The stability of the working conditions is assured by selecting, from registered data, a period of time (20 min at least) in which temperatures, pressure and both  $\dot{m}_{weak}$  and  $\dot{m}_{strong}$  show a constant behaviour. With these ranges for reference, the stability of the remaining variables is checked.

After this procedure, the recorded data corresponding to all sensors connected to the data loggers is averaged. Table 2 presents sensors used in the experimental test facility.

#### EXPERIMENTAL UNCERTAINTY ANALYSIS

A calibration process was carried out for all instruments described in Figure 1. Using the calibration functions for every sensor, systematic errors were reduced as much as possible. The remaining random uncertainty U for an experimental result R, which is a function

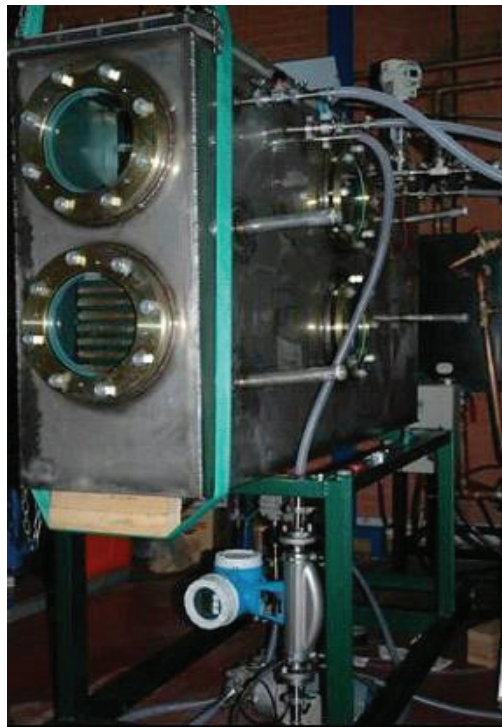


Figure 2. Images of the absorption test facility

Table 1. Operating ranges of input variables

Parameter	Working Range
Inlet oil temperature ( $t_{set}$ )	78.8 – 99 °C
Weak solution mass flow rate ( $\dot{m}_{weak}$ )	169.6-363.5 kg/h
Recirculated solution mass flow rate ( $\dot{m}_r$ )	261.8-1051.3 kg/h
Cooling water temperature, condenser	18.9-30.8 °C
Cooling water temperature, subcooler	18.5-30.1 °C
Chilled water temperature, evaporator 1	6.5-19.1 °C
Chilled water temperature, evaporator 2	9.7-19.8 °C
Refrigerant outlet temperature, condenser	17-28 °C
Refrigerant inlet temperature, evaporator 1	18.3-23.6 °C
Refrigerant inlet temperature, evaporator 2	15.4-21.3 °C
Refrigerant outlet pressure, condenser	2.8-5.9 kPa
Low pressure	0.7-1.9 kPa

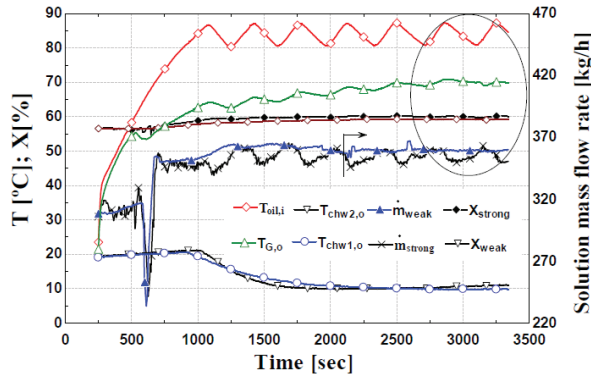


Figure 3. Temperatures, concentration and flow rates vs. time during an experiment

Table 2. Sensors used in the experimental test facility

Instrument	Quantity	Range	Uncertainty
Thermocouple	30	5 - 110 °C	±(0.2°C - 0.6°C)
Solution flow and density meter	2	150-400 kg/h	± 0.5%
Oil flowmeter	1	1000-3600 l/h	± 3.1%
Cooling water flowmeters	2	1200-1500 kg/h	± 1.1%
Recirculated solution flowmeters	1	200-1000 kg/h	± 1.3%
Fan coil flowmeters	2	400-600 kg/h	± 0.7%
Pressure sensors	4	7-130 mbar	±(1.8 - 3)%

of  $n$  independent parameters  $x_i$ , is estimated, according to the Gauss algorithm, as:

$$U = \sqrt{\sum_{i=1}^n \left( \frac{\partial f}{\partial x_i} \cdot u_{x_i} \right)^2}, \quad R = f(x_1, x_2, \dots, x_n) \quad (1)$$

The uncertainty of instruments is given in Table 2.

### RELEVANT PARAMETERS

The performance parameters corresponding to each one of the operating conditions are obtained according to the procedure explained in the previous section.

From measured values of inlet (*i*) and outlet (*o*) water temperatures *t* of both evaporators, cooling power is obtained from Eq. (2):

$$\dot{Q}_E = \dot{m}_{chw} \cdot C_w \cdot (t_{chw,i} - t_{chw,o}) \quad (2)$$

The heating power supplied to the generator was calculated as:

$$\dot{Q}_G = \dot{m}_{oil} \cdot C_{oil} \cdot (t_{oil,i} - t_{oil,o}) \quad (3)$$

C corresponds specific heat capacity of a liquid and *m* is the mass flow rate. The subscript “chw” corresponds to chilled water.

The experimental COP was calculated as the quotient of (2) and (3).

$$COP = \frac{\dot{Q}_E}{\dot{Q}_G} \quad (4)$$

In this work, the selection of variables involved in the obtaining of an ANN model is based on the proved dependency of the facility performance with external water circuit temperatures and the “overflow” of refrigerant in the evaporators (Gutiérrez *et al.*, 2012). The overflow depends on the internal fluid temperatures of the liquid refrigerant at the condenser exit and the evaporators entries  $T_{l,C}$ ,  $T_{l,E1}$ ,  $T_{l,E2}$ , as well as the low pressure  $P_{low}$  and condenser exit pressure  $P_{C,o}$ . Therefore, the input layer consists of 8 temperatures: The external fluid circuit temperatures in the generator, sub-cooler, condenser, and evaporators  $T_{G,set}$ ,  $T_{cw,C}$ ,  $T_{chw,E1}$ ,  $T_{chw,E2}$  respectively, and the above mentioned  $T_{l,C}$ ,  $T_{l,E1}$ ,  $T_{l,E2}$ . In addition, 2 mass flow rates, corresponding to weak and re-circulated solutions,  $\dot{m}_{weak}$  and,  $\dot{m}_r$ , which are controlled variables. Finally,  $P_{low}$  and  $P_{C,o}$  are also included. In sum 12 input operation variables will be considered in the artificial neural model.

Another model was developed based on the principle of the accessibility of data in practical applications, with the intention that such model could be used as a black box. The variables selected for this scenario are the mean value of external fluid circuit temperatures:  $T_{G,set}$ ,  $T_{cw,C}$ ,  $T_{chw,E1}$ ,  $T_{chw,E2}$ . Time is also included in this study in order to compare the simulated and experimental data in a transient experiment.

The output layer contains only one of the three variables: the generation power ( $\dot{Q}_G$ ), the cooling power ( $\dot{Q}_E$ ), or the COP.

## ARTIFICIAL NEURAL NETWORKS MODEL

Neurons are grouped into distinct layers (input, hidden and output layer) as well as interconnected according to a given architecture. The network function is determined largely by the connections between neurons. Normally, each connection between two neurons has a weight and bias coefficients attached to it. The standard network structure for an approximation function is the multiple-layer feed forward which has one or more hidden layers of sigmoid neurons followed by an output layer of linear neurons.

The linear output layer lets the network produce values outside the -1 to +1 range. The linear output layer function is used for forecasting the performance of the adiabatic absorption cycle (Hernandez *et al.* 2009b).

### LEARNING ALGORITHM

The learning algorithm is defined as a procedure that involves adjusting of the weights and biases, by minimizing an error function (usually a quadratic one) between the network output, for a given set of inputs, and the correct target. If smooth non-linearity is applied, the gradient of the error function can be computed by the classical back-propagation procedure (Natricks *et al.*, 1998). In this work, the Levenberg-Marquardt algorithm optimization procedure –in the Matlab Neural Network Toolbox was used. This algorithm is an approximation of Newton’s method which was designed to approach second order training speed without having to compute the Hessian matrix (Martin *et al.*, 1994). The root mean square error (RMSE) is calculated with the theoretical values and network predictions.

### DATABASE PREPARATION

Steady states and transitory data were considered for the absorption system modelling by means of artificial neural networks. In order to characterize the system, 219 experimental points were obtained at different operating conditions (Table 1). These data was used to train and test the steady state and transient ANN models. For transient data base 1445 values were considered for a period of time.

In order to test the robustness and then the prediction ability of the models, the experimental database was split into the learning and testing database. Both transient and steady state experimental database were split into learning (80% of the data) and testing (20% of the data) with the objective of obtaining the best correlation between output target and output simulation

and a good representation of the operating performance. With the learning database the optimal weights and biases are obtained and with the testing database the model is validated (Rumelhart *et al.*, 1986). The model adequacy is obtained after testing the increment of neurons in the hidden layer. In this model, we avoided over-fitting by considering the comparison between the root mean square error (RMSE) obtained for both the learning database and the testing database (Hernández *et al.*, 2009b).

The input layer consists of variables that the operator can control and/or that influence the equipment performance. In response to this, variables selected correspond to those listed in section 4. Input and output parameters were normalized for calculation from 0 to 1 (Khataee and Mirzajani, 2010).

#### INVERSE ARTIFICIAL NEURAL NETWORK

According to Hernández (2009); Labus *et al.* (2012); Hernández *et al.* (2012); Laidi and Hanin, (2013); Hernández (2013); Morales *et al.* (2015); the artificial neural network can be inverted to calculate a desired input parameter. In order to apply this inverse artificial neural network (ANNi), first it is necessary to have the ANN model. In this case, the multi-layer feed-forward (MLFF) is applied. If the hyperbolic tangent sigmoid transfer function is used in the hidden layer and the linear function is considered in the output layer then the output layer is:

$$Output = \sum_{j=1}^S \left[ W_o(j) \cdot \left( \frac{2}{1 + \exp(-2 \cdot (\sum_{k=1}^K (W_i(j,k) \cdot \ln(k)) + b1_{(j)}))} - 1 \right) \right] \quad (5)$$

Where:

- $ln(k)$  = the inputs parameters
- $W_i$  = the weight between input and hidden layer
- $W_o$  = the weight between hidden and output layer
- $b1$  = the bias in the hidden layer and
- $b2$  = the bias in the output
- $S$  = the neurons number in the hidden layer
- $k$  = the parameters number in the input layer

Consequently, if the Equation 5 has more of one neuron in the hidden layer ( $S > 1$ ), then the inverse artificial neural network can be as following (Hernández, 2009a) equation 6.

$$Fun_{ln(x)} = b2 - \sum_{j=1}^S W_o(j) - Output + \sum_{j=1}^S \left[ \frac{2W_o(j)}{1 + \exp(-2(W_i(j,x) \cdot \ln(x) + \sum_{k=1, k \neq x}^K (W_i(j,k \neq x) \cdot \ln(k \neq x)) + b1_{(j)}))} \right] \quad (6)$$

Where  $ln(x)$  is the input parameter value to be calculated. Consequently, the Equation (6) can be solved using a method of optimization to obtain the desired input parameter. In this case, the Nelder-Mead simplex algorithm was applied.

In the case that the Equation 5 had only one neuron in the hidden layer then it can have an analytical solution (Hernández, 2009b).

#### RESULTS AND DISCUSSION

In this work, three neural network models were obtained from different configuration applied. First, steady state database was worked to obtain  $\dot{Q}_G$  and  $\dot{Q}_E$  prediction. The architecture of a neuronal network model is the following: 12 input neurons with 2 neurons in the hidden layer (involving 29 coefficients: 26 weight and 3 biases). This structure was found to be efficient in predicting  $\dot{Q}_G$ . The same operation variables in the input layer were used to predict  $\dot{Q}_E$ . For this model, 3 neurons in the hidden layer were found to be satisfactory. The neural network model developed (Figure 4) involved three and two neurons to determine  $\dot{Q}_E$  and  $\dot{Q}_G$ , respectively, for a steady state condition.

The input layers for these neural network models are also illustrated in this Figure 4. Table 3 shows the main characteristics of how neural network models work.

The comparison of experimental  $\dot{Q}_E$  and  $\dot{Q}_G$  against simulated results using ANN models, for steady state data are illustrated in Figures 6a and 6b. Satisfactory results ( $R > 0.98$ ) were obtained in both cases. Experimental and simulated data of  $\dot{Q}_E$  values were compared through a linear regression model in Figure 6a ( $\dot{Q}_{Esim} = a + b\dot{Q}_{Eexp}$ ;  $n = 219$ ;  $R = 0.9867$ ; confidence level  $>99\%$ ) (Bevington and Robinson, 2003; Verma, 2005). The intercept  $a$  ( $-0.0331 < a < 0.0443$ ) includes zero, and the slope  $b$  ( $0.9646 < b < 1.0223$ ) includes 1. For the case of,  $\dot{Q}_G$  results are illustrated in Figure 5 ( $\dot{Q}_{Gsim} = a + b\dot{Q}_{Gexp}$ ;  $n = 219$ ;  $R = 0.9879$ ). The intercept  $a$  ( $-0.0229 < a < 0.1881$ ) includes zero, and the slope  $b$  ( $0.9553 < b < 1.0098$ ) includes 1. Both models indicate statistically significant correlation between the experimental and simulated heat flux values without any bias (Verma, 2005). Consequently, neural network was validated with the actual steady state database. The proposed artificial neural network matches very well the whole database, thus simplifying the energy analysis.

Regarding the results for transient data, the architecture of neural networks keeps the same input layer

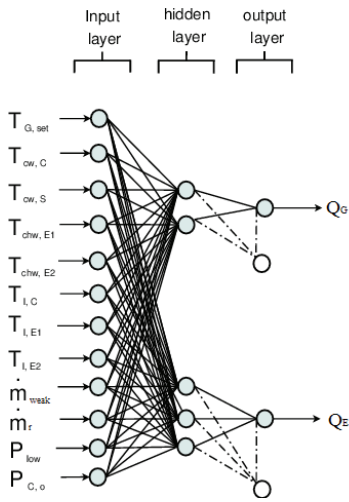


Figure 4. Input and output variables used for the neural network computational model

Table 3. Artificial neural networks models development in this work

$\phi$	N° of neurons in the input layer	N° neurons in the hidden layer	Output layer	R	Intercept	Slope
Model 1 (steady state)	12	3	$Q_E$	0.9867	0.0056	0.9934
Model 2 (steady state)	12	2	$Q_G$	0.9879	0.0826	0.9826
Model 3 (dynamic state)	12	12	$Q_E$	0.9648	0.0738	0.9470
Model 4 (dynamic state)	12	16	$Q_G$	0.9790	0.1659	0.9653

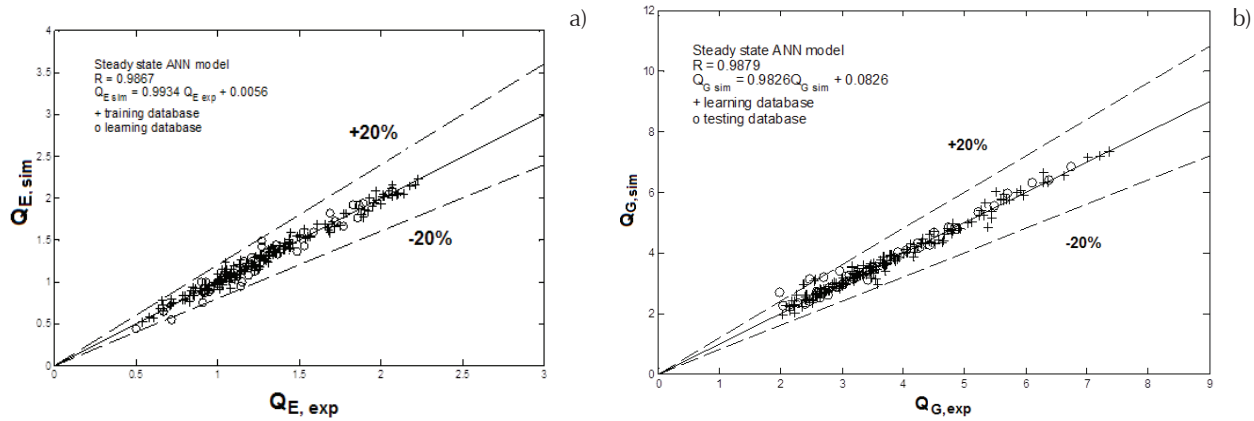


Figure 5. Experimental and simulated values of evaporator power  $\dot{Q}_E$  and generator power  $\dot{Q}_G$  using steady state database, a) results for  $\dot{Q}_E$ , b) results for  $\dot{Q}_G$

in this work using 12 operation variables. Experimental and simulated data of  $COP$  values were compared through a linear regression model in Figure 6. Again, satisfactory results were obtained with  $R > 0.98$  ( $COP = a + bCOP_{exp}$ ;  $n = 1562$ ;  $R = 0.9911$ , confidence level  $> 99\%$ ) (Bevington and Robinson, 2003; Verma, 2005).

The intercept  $a$  ( $-0.0011 < a < 0.0057$ ) includes zero, and the slope  $b$  ( $0.9837 < b < 1.0010$ ) includes 1. Consequently, the statistical significant correlation between experimental and simulated values at transient conditions was found.

The results corresponding to the additional model developed for transient data, which includes only the temperatures of external fluid circuits, are depicted in Figure 7a. In order to predict the coefficient performance 32 neurons in a hidden layer were necessary. The hyperbolic tangent sigmoid transfer function (tan sig) and a linear function were used to obtain the resulting model. The variation of  $COP$  with time corresponds to the behavior of experimental data shown in Figure 3, due to the on-off control. Figure 7b shows the relative error obtained, which is less than 10% for most data. These are satisfactory results and demonstrate that the ANN approach is appropriate for the performance prediction of absorption systems using available data. Other objectives such as absorption machine control as well as optimization can also be met.

Even though the dynamic behavior of a thermal device is complicated, the results obtained using an ANN analysis in a transient model were good. This tool allows us to determine a real-time coefficient of perfor-

mance in order to make the necessary adjustments to optimize the operation of an absorption facility.

### OPTIMUM OPERATING CONDITIONS USING INVERSE NEURAL NETWORK

According to the artificial neural network section presented in this work, it is possible to propose an online estimation strategy of the  $COP$ . The following steps were developed: First, it is possible to predict the coefficient of performance considering only external variables in the system. The temperatures at generator, condenser and temperatures corresponding to evaporator 1 and 2 were selected in this section. Second, training and validation of ANN model to predict the  $COP$  in transient state. The training procedure was carried out following the steps enlisted previously in the artificial neural network section. The ANN trained had 32 neurons in the hidden layer and  $T_{cw,C}$ ,  $T_{cw,S}$ ,  $T_{E1}$ ,  $T_{E2}$ , and time as the neurons in the input layer to predict  $COP$ .

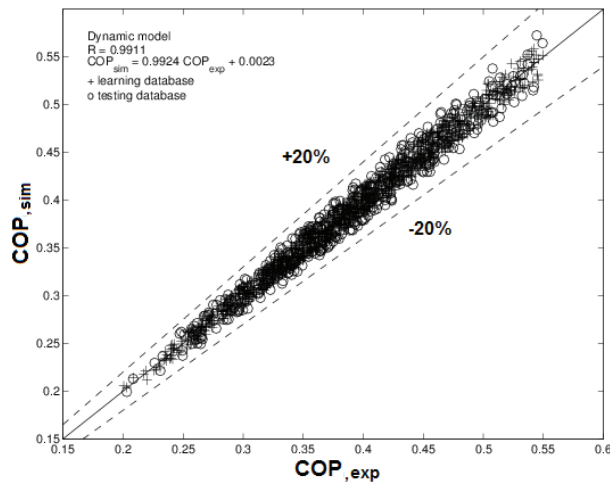


Figure 6. Experimental and simulated values corresponding to coefficient of performance using the dynamic database

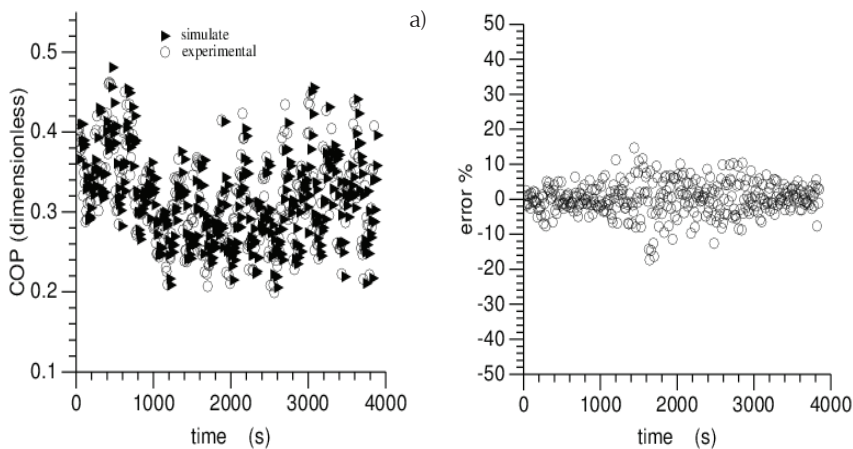


Figure 7a. Experimental and simulated values of coefficient of performance  $COP$  vs. time using transient database  
Figure 7b. Relative error between simulated and experimental values of  $COP$  vs. time using transient database

Experimental and simulated data of COP values were compared through a linear regression model in Figure 8 as:  $OP = 0.0169 + 0.9427COP_{exp}$ ,  $R = 0.9696$  and  $n = 385$ . Therefore, the capacity of such model to predict the COP in transient state has been verified.

Finally, the artificial neural network inverse as optimization strategy. In addition to this, a strategy for optimizing the COP for the system has been developed. The selected strategy is the inverse neural network. With the aim of developing the artificial neural network to the experimental facility presented in this work, a test is carried out.

The direct neural network model is used to estimate the COP, based on the following operating conditions:  $T_C = 21.93$  °C,  $T_S = 21.34$  °C,  $T_{E1} = 15.77$  °C,  $T_{E2} = 16.18$  °C. The generator temperature is estimated as a function of time according to the following relationship:

$$T_G = 0.00747t + 85 \quad (7)$$

Equation (7) is used to reproduce the generator temperature  $T_G$  versus time (t), keeping fixed operating condi-

tions. Figure 9 shows the COP against time as the result of simulation of the direct neural network.

The inverse neural network is developed based on the following expression (Hernández, 2009b):

$$f(Tg) = b_{2(1,1)} - \sum_{j=1}^s W_o(j) - COP + \sum_{j=1}^s \left[ \frac{2W_{o(1,j)}}{1 + e^{-2(y_j + w'_{j,1})Tg}} \right] \quad (8)$$

Where  $s$  is the number of hidden neurons and  $y_i$  estimated as:

$$y_j = -2(W_{i(j,2)} T_{cw,C} + W_{i(j,3)} T_{cw,S} + W_{i(j,4)} T_{E1} + W_{i(j,5)} T_{E2} + W_{i(j,6)} T_{1,C} + W_{i(j,7)} T_{E1} + W_{i(j,8)} T_{1,E2} + W_{i(j,9)} \dot{m}_{weak} + W_{i(j,10)} \dot{m}_r + W_{i(j,11)} P_{low} + W_{i(j,12)} PC_o + b_{1(j,1)}) \quad (9)$$

Weights and bias are obtained from direct neural network model.

It is possible to obtain the time when the system reaches the experimental point  $COP=0.3115$ . The numerical result obtained is  $t=503.8750$  using the inverse neural network inverse methodology. The relative absolute percentage error calculated is 0.775% compared to time

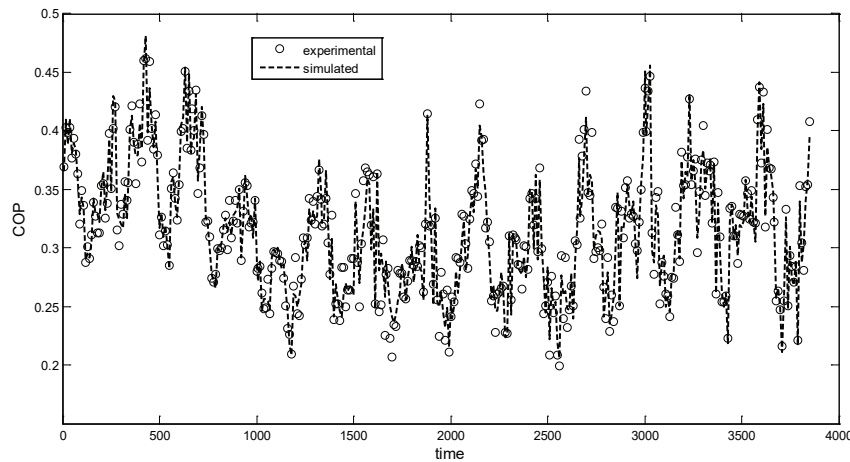


Figure 8. Transcendent experimental data to train and validate the direct ANN model

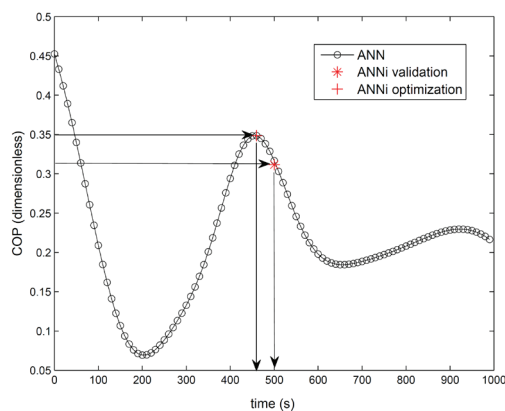


Figure 9. Coefficients of performance against time simulated with the direct ANN

experimentally determined. The error is calculated as follows:

$$U = \frac{|exp - sim|}{exp} \times 100 \quad (10)$$

The computation time to solve the inverse neural network was 4.04 s.

However, the process could be reaching to a new stable state, or at least that indicates the simulation. In order to estimate the optimum *COP*, the inverse neural network strategy was applied for a second time. Assuming an optimal *COP* = 0.3485 (see Figure 8), keeping the operating conditions described above, the time in which the system reaches the optimum value is calculated. The calculated time with the artificial neural network is  $t = 476.5_s$ . The percentage error calculated was 3.59% compared to the time estimated using the direct neural network.

### CONCLUSIONS

The application of artificial neural networks for modeling the performance of a particular adiabatic absorption facility has been developed in this work. Experimental results are included in steady and transient operations. Three models were obtained corresponding to cooling and generation capacities and coefficient of performance of the experimental system. These models were trained and validated with both steady and transient state experimental database. With the purpose of using a black-box model, an additional model was obtained using external circuit temperatures, with satisfactory results when compared in a transient experiment. Results demonstrated a good agreement between experimental and simulated values for all cases. The models obtained could be used to predict cycle performance or on-line estimation. Optimization of *COP* was carried out using an inverse neural network with satisfactory results. This method, applied to transient data, demonstrate to be a useful tool for control purposes.

### ACKNOWLEDGMENTS

The authors want to express their gratitude to the Universidad Autónoma de San Luis Potosí (UASLP) for the support given through PROMEP, project N° 103.5/13/6575. The financial support of this study by the Spanish Ministry of Education, Science and Technology

through CLIMABCAR project DPI 2003-01567 is greatly appreciated.

### REFERENCES

- Afram A., Janabi-Sharifi F., Fung A.S. and Raahemifar K. (2017). Artificial neural network (ANN) based model predictive control (MPC) and optimization of HVAC systems: A state of the art review and case study of a residential HVAC system. *Energy and Buildings*, 141 (15), 96-113. <https://doi.org/10.1016/j.enbuild.2017.02.012>
- Álvarez M.E., Hernández J. and Bourouis M. (2016). Modelling the performance parameters of a horizontal falling film absorber with aqueous (lithium, potassium, sodium) nitrate solution using artificial neural networks. *Energy*, 102, 313-323. <https://doi.org/10.1016/j.energy.2016.02.022>
- Arcaklioglu, E. (2004). Performance comparison of CFCs with their substitutes using artificial neural network. *International Journal of Energy Research*, 28, 1113-1125. <https://doi.org/10.1002/er.1020>
- Bevington, P. and Robinson, D. (2003). *Data reduction and error analysis for the physical science*. 3rd. Ed. New York, USA: McGrawHill.
- Colorado D., Hernández J., Rivera W., Martínez H. and Juárez D. (2011). Optimal operation conditions for a single-stage heat transformer by means of an artificial neural network inverse. *Applied Energy*, 88(4), 1281-1290. <https://doi.org/10.1016/j.apenergy.2010.10.006>
- Chow, T., Zhang, G., Lin, Z. and Song, C. (2002). Global optimization of absorption chiller system by genetic algorithm and neural network. *Energy and Buildings*, 34(1), 103-109. [https://doi.org/10.1016/S0378-7788\(01\)00085-8](https://doi.org/10.1016/S0378-7788(01)00085-8)
- Florides, G., Kalogirou, S., Tassou, S. and Wrobel, L. (2003). Design and construction of a LiBr-water absorption machine. *Energy Conversion and Management*, 44(15), 2483-2508. [https://doi.org/10.1016/S0196-8904\(03\)00006-2](https://doi.org/10.1016/S0196-8904(03)00006-2)
- Gutiérrez-Urueta, G., Rodríguez, P., Venegas, M., Ziegler, F. and Rodríguez-Hidalgo, M. (2011). Experimental performances of a LiBr-water absorption facility equipped with adiabatic absorber. *Int. J. Refrigeration*, 34(8), 1749-1759. <https://doi.org/10.1016/j.ijrefrig.2011.07.014>
- Gutiérrez-Urueta, G., Rodríguez, P., Ziegler, F., Lecuona, A. and Rodríguez-Hidalgo, M. (2012). Extension of the characteristic equation to absorption chillers with adiabatic absorbers. *Int. J. Refrigeration*, 35(3), 709-718.
- Gutiérrez, G., Venegas, M., Rodríguez, P., Izquierdo, M. and Lecuona, A. (2006). Experimental characterization of a single stage LiBr-H<sub>2</sub>O absorption test rig. Proceedings of. ECOS. Vol. 3, 1311-1316, *Conference in Crete, Greece*.
- Hellmann, H.M., Schweigler, C. and Ziegler, F. (1998). A simple method for modeling the operating characteristics of absorption chillers. *Proceedings of Thermodynamics heat and mass trans-*

- fers of refrigeration machines and heat pumps seminar EUROtherm No 59, Seminar in Nancy, France.
- Hernández J.A. (2009). Optimum operating conditions for heat and mass transfer in foodstuffs drying by means of neural networks inverse. *Food Control*, 20, 435-438. <https://doi.org/10.1016/j.foodcont.2008.07.005>
- Hernández, J.A., Bassam, A., Siqueiros, J. and Juárez-Romero, D. Optimum operating conditions for a water purification process integrated to a heat transformer with energy recycling using neural network inverse. *Renewable Energy*, 34, 1084-1091. <https://doi.org/10.1016/j.renene.2008.07.004>
- Hernández J.A., Colorado D, Cortés-Aburto O, El Hamzaoui Y, Velázquez V.M and Alonso B. (2013). Inverse neural network for optimal performance in polygeneration systems. *Applied Thermal Engineering*, 50, 1399-1406. <https://doi.org/10.1016/j.applthermaleng.2011.12.041>
- Hernández, J.A., Rivera, W., Colorado, D. and Moreno-Quintanar, G. (2012). Optimal COP prediction of a solar intermittent refrigeration system for ice production by means of direct and inverse artificial neural networks. *Solar Energy*, 86(4), 1108-1117. <https://doi.org/10.1016/j.solener.2011.12.021>
- Hosoz, M. and Ertunc, H. M. (2006). Modeling of a cascade refrigeration system using artificial neural network. *International Journal of Energy Research*, 30, 1200-1215. <https://doi.org/10.1002/er.1218>
- Joudi, K.A. and Lafta, A.H. (2001). Simulation of a simple absorption refrigeration system. *Energy Conversion and Management*, 42(13), 1575-1605. [https://doi.org/10.1016/S0196-8904\(00\)00155-2](https://doi.org/10.1016/S0196-8904(00)00155-2)
- Khataee A.R. and Mirzajani O. (2010) UV/peroxydisulfate oxidation of C.I. basic blue 3: modeling of key factors by artificial neural networks. *Desalination*, 251, 64-69. <https://doi.org/10.1016/j.desal.2009.09.142>
- Kumar K.V., Paradeshi L., Srinivas M. and Jayaraj S. (2016). Parametric Studies of a Simple Direct Expansion Solar Assisted Heat Pump Using ANN and GA. *Energy Procedia*, 90, 625-634. <https://doi.org/10.1016/j.egypro.2016.11.231>
- Labus, J., Bruno, J.C. and Coronas, A. (2010). Performance analysis of small capacity absorption chillers by using different modeling methods. *Applied Thermal Engineering*, 58(1-2), 305-313. <https://doi.org/10.1016/j.applthermaleng.2013.04.032>
- Labus, J., Hernández, J.A., Bruno, J.C. and Coronas, A. Inverse neural network based control strategy for absorption chillers. *Renewable Energy*, 39, 471-482, 2012. <https://doi.org/10.1016/j.renene.2011.08.036>
- Laidi, M. and Hanin, S. (2013). Optimal solar COP prediction of a solar-assisted adsorption refrigeration system working with activated carbon/methanol as working pairs using direct and inverse artificial neural network. *International Journal of Refrigeration*, 36, 247-257. <https://doi.org/10.1016/j.ijrefrig.2012.09.016>
- Manohar, H.J., Saravanan, R. and Renganarayanan, S. (2006). Modeling of steam fired double effect vapour absorption chiller using neural network. *Energy Conversion and Management*, 47(15-16), 2202-2210. <https://doi.org/10.1016/j.enconman.2005.12.003>
- Martin, T., Hagan, M.T. and Mohammad, B.N. (1994). Training Feedforward networks with the Marquardt algorithm. *IEEE Transactions on Neural Networks*, 6, 989-993. <https://doi.org/10.1109/72.329697>
- Mohanraj, M., Jayaraj, S. and Muraleedharan, C. (2009). Exergy analysis of direct expansion solar-assisted heat pumps using artificial neural networks. *International Journal of Energy Research*, 33(11), 1005-1020. <https://doi.org/10.1002/er.1534>
- Mohanraj, M., Jayaraj, S. and Muraleedharan, C. (2012). Applications of artificial neural networks for refrigeration, air-conditioning and heat pump systems—A review. *Renewable and Sustainable Energy Reviews*, 16(2), 1340-1358. <https://doi.org/10.1016/j.rser.2011.10.015>
- Morales L.I., Conde-Gutiérrez R.A., Hernández J.A., Huicochea A., Juárez-Romero D. and Siqueiros J. (2015). Optimization of an absorption heat transformer with two-duplex components using inverse neural network and solved by genetic algorithm. *Applied Thermal Engineering*, 85, 322-333. <https://doi.org/10.1016/j.applthermaleng.2015.04.018>
- Natricks, M. A., Demuth, H. and Beale, M. (1998). *Neural network toolbox for Matlab-User's Guide*. The Math Works Inc. [http://cda.psych.uiuc.edu/matlab\\_pdf/nnet.pdf](http://cda.psych.uiuc.edu/matlab_pdf/nnet.pdf)
- Rosiek, S. and Batlles, F. J. (2010). Modelling a solar-assisted air-conditioning system installed in CIESOL building using an artificial neural network. *Renewable Energy*, 35, 2894-2901. <https://doi.org/10.1016/j.renene.2010.04.018>
- Rumelhart, D.E., Hinton, G.E. and Williams, R. J. (1986). Learning internal representations by error propagation. *Parallel data processing 1*, 318-362, MA, USA, MIT Press Cambridge.
- Şencan, A. (2007). Performance of ammonia-water refrigeration systems using artificial neural networks. *Renewable Energy*, 32(2): 314-328. <https://doi.org/10.1016/j.renene.2006.01.003>
- Şencan, A. and Kalogirou, S.A. (2005). A new approach using artificial neural networks for determination of the thermodynamic properties of fluid couples. *Energy Conversion and Management*, 46(15-16), 2405-2418. <https://doi.org/10.1016/j.enconman.2004.11.007>
- Şencan, A., Yakut, K.A. and Kalogirou, S.A. (2006). Thermodynamic analysis of absorption systems using artificial neural network. *Renewable Energy*, 31, 29-43. <https://doi.org/10.1016/j.renene.2005.03.011>
- Sözen, A. and Akçayol, M. A. (2004). Modelling (using artificial neural-networks) the performance parameters of a solar-driven ejector-absorption cycle. *Applied Energy*, 79(3), 309-325. <https://doi.org/10.1016/j.apenergy.2003.12.012>
- Sözen, A., Arcaklioglu, E. and Mehmet, Ö. (2003). A new approach to thermodynamic analysis of ejector-absorption cycle: artificial neural networks. *Applied Thermal Engineering*, 23(8): 937-952. [https://doi.org/10.1016/S1359-4311\(03\)00034-6](https://doi.org/10.1016/S1359-4311(03)00034-6)

- Sözen, A., Arcaklioğlu, E. and Özalp, M. (2004). Performance analysis of ejector absorption heat pump using ozone safe fluid couple through artificial neural networks. *Energy Conversion and Management*, 45(13-14), 2233-2253. <https://doi.org/10.1016/j.enconman.2003.11.002>
- Tugcu A. and Arslan O. (2017). Optimization of geothermal energy aided absorption refrigeration system-GAARS: A novel ANN-based approach. *Geothermics*, 65, 210-221. <https://doi.org/10.1016/j.geothermics.2016.10.004>
- Verma, S.P. (2005) *Estadística básica para el manejo de datos experimentales: aplicaciones en Geoquímica (Geoquimiometría)*. 1st ed. México: Universidad Nacional Autónoma de México.
- Yung, C.C. (2007). Sequencing of chillers by estimating chiller power consumption using artificial neural networks. *Building and Environment*, 42(1), 180-188. <https://doi.org/10.1016/j.buildenv.2005.08.033>